

# Chapter 2

## Microfluidic Technologies and Platforms for Protein Crystallography



Masatoshi Maeki and Manabu Tokeshi

**Abstract** Protein crystallization and its three-dimensional structure analysis is indispensable for understanding the protein function in the body and life phenomenon. Three dimensional structure of protein also plays important role for drug discovery and it have been already used to design new drug. To determine the three dimensional protein structure, protein crystallization conditions: concentration of protein, kinds and concentration of precipitant, buffer, pH, temperature, and additives must be optimized. In addition, high-diffraction quality protein crystals are needed to determine the protein three-dimensional structure at high resolution. However, optimization of the protein crystallization condition and preparation of high quality protein crystals require the labor intensives and trial-and-error. Microfluidics can provide the solution for the problems of traditional protein crystallography. A lot of microfluidic based technologies and platforms have been developed to utilize their unique characteristics. In this chapter, microfluidic technologies and platforms for protein crystallography is summarized. In particular, the application of microfluidics for high-throughput protein crystallization condition screening, controlling of protein crystal growth, and on-chip X-ray diffraction experiment using microfluidic devices are overviewed.

**Keywords** Protein crystallography · Droplet microfluidics · Normally-closed valve · Crystal growth · X-ray crystal structure analysis

### 2.1 Introduction

Biological sample is valuable and expensive due to the difficulty of sample preparation acquired from human patients, animals, cells, and bacteria. The acquired sample contains many impurities, which have to remove by appropriate pretreatment methods for each clinical diagnosis, assay, or experiment. In the pretreatment step,

---

M. Maeki (✉) · M. Tokeshi  
Division of Applied Chemistry, Faculty of Engineering, Hokkaido University, Sapporo, Japan  
e-mail: [m.maeki@eng.hokudai.ac.jp](mailto:m.maeki@eng.hokudai.ac.jp)

the target biological molecules isolate from the impurities using separation techniques such as, centrifuge, electrophoresis, and chromatography. Generally, the purification step requires multiple trials with different separation modes [1, 2]. In the case of protein purification, affinity chromatography is the first choice for tag-fusion proteins. After the affinity chromatography, ion exchange chromatography and gel filtration chromatography are considered to obtain the high purity protein sample. When we need a large amount or high concentration of target protein sample, a scale scale-up of purification volume is required, because protein cannot be amplified unlike the nucleic acids. In particular, preparation of membrane protein is more complicated compared with soluble protein. From these reasons, preparation of the high purity biological sample is labor-intensive and time-consuming process.

Microfluidic technologies and platforms can offer many advantages in biological applications [3–6]. Reduction of sample consumption, high-throughput screening, shortening detection time, distinguishing fluid characteristic are remarkable features of microfluidic devices, and it facilitate the cell separation and single cell analysis [7–9], biological assays [10–12], pharmaceuticals [13–15], drug screening [16–18]. These are essential and powerful features for the biological applications, especially for protein analysis, because the high purity protein sample is valuable and expensive.

In the field of protein analysis, structure biology is a key research area to elucidate the relationship between the protein structure and the protein function [19–21]. Protein can function by precisely folding into its native “three-dimensional” structure. Conversely, misfolded proteins not only lose a function but also cause of the disease like an amyloidosis [22]. Determination of the protein three-dimensional structure provides us the essential information including protein-protein interaction, active site of protein, and protein-ligand binding site. The protein structural information is indispensable for the structure based drug design and development of molecularly-targeted therapy [23–25]. To determine the protein three-dimensional structure, X-ray crystallography [26–28], nuclear magnetic resonance spectroscopy (NMR) [29], and cryo-electron microscopy (cryo-EM) [30] are gold standard analytical methods. Although these are powerful analytical methods for protein structure and dynamics measurement, 80 ~ 90% of protein structures have been determined by X-ray crystallography.

In the protein X-ray crystallography, the preparation of high quality protein crystals is remaining problem to determine the precise three-dimensional protein structure. After the purification step, screening of the protein crystallization conditions is carried out by the conventional protein crystallization method, such as the hanging drop vapor diffusion method, sitting drop vapor diffusion method, microbatch method, and liquid-liquid interface diffusion method, as shown in Fig. 2.1 [31]. At the primary screening, the kinds and concentration of precipitant solution, concentration of protein solution, kinds, pH, and concentration of buffer solution, crystallization temperature, and additives are optimized to obtain protein crystals. We can roughly predict the suitable crystallization condition from the homology of proteins, which have been recorded in the Protein Data Bank (PDB). However, protein crystals do not always appear the similar crystallization condition.

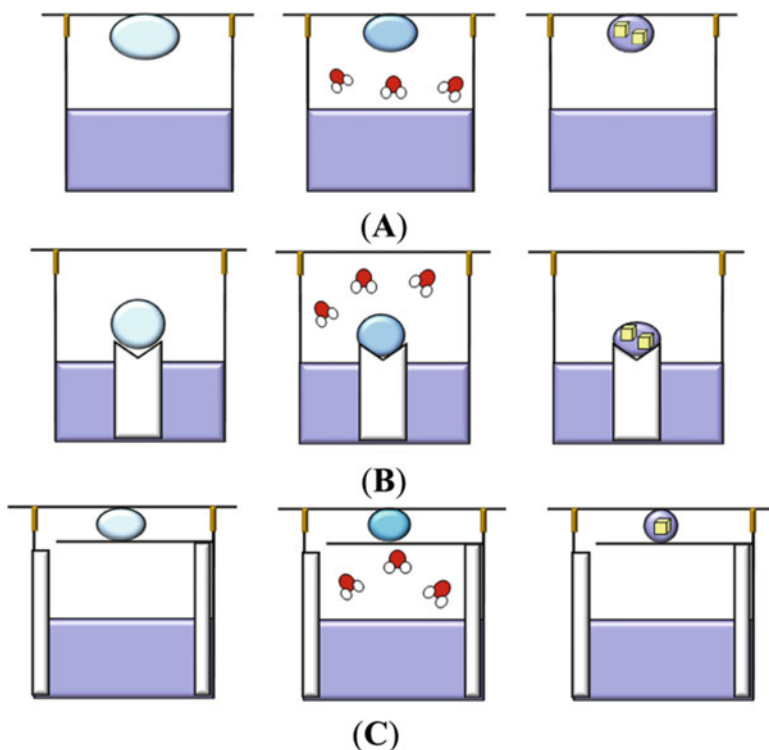


**Fig. 2.1** Schematic illustrations of the conventional protein crystallization methods. Vapor diffusion method. A drop containing unsaturated precipitant and protein solution is placed in a crystallization well containing a precipitant solution. The well is sealed with grease to prevent evaporation and to allow vapor equilibration of the droplet and the reservoir. Equilibration of water vapor from the protein-containing droplet to the reservoir solution causes the protein solution to reach a supersaturation level, where nucleation and initial growth occur. **(A)** Hanging drop vapor diffusion method. **(B)** Sitting drop vapor diffusion method. **(C)** Sandwich drop vapor diffusion method. (Reprinted with permission from Ref. [31] with permission from MDPI)

Therefore, a comprehensive trial is unavoidable at the primary screening experiment. Typically,  $1 \sim 2 \mu\text{L}$  of protein solution is needed for one trial, and thus, a several hundred microliter valuable protein solution is required for the comprehensive crystallization condition screening.

Then the secondary screening is conducted based on the results of primary screening to obtain high quality protein crystals. Although optimization of the crystallization condition is significant, the control of protein crystal growth is indispensable factor for obtaining the high quality of protein crystals. Growth control of the crystal regardless of the proteins or inorganic materials, at the ground environment is attracted in many researchers for improving the molecular packing. Formation of the natural convection is the major reason to disrupt the ordered molecular packing of crystal at the ground environment. For improving the quality

of crystals, the microgravity, electric field, and magnetic field are used to control the crystal growth environment, even though specialized experimental apparatus are required [32–37].

Microfluidic technologies and platforms can resolve the abovementioned problems using its unique characteristics [38–41]. Reduction of the protein consumption is easily achievable by downsizing of the device dimension. Only nano to picoliter volume of protein solution is needed for one trial, and the microfluidic device enables the high-throughput screening of protein crystallization condition [42–54]. In addition, the “micro-sized crystallization space” allow the control of protein crystal growth different from the conventional crystallization environment [55–61]. In this chapter, microfluidic techniques and platforms for protein crystallography to accelerate the field of structural biology are summarized and the applications of microfluidic devices combined with the recent synchrotron facilities are also overviewed.

## 2.2 Principle of the Protein Crystallization and X-Ray Diffraction Measurement

In brief, the protein crystallization experiment constructs: screening of protein crystallization condition, preparation of high quality protein crystal, screening of cryoprotection condition, and X-ray diffraction measurement. In the case of conventional methods, a micropipette is used to prepare the protein crystallization screening setups. Generally, 1  $\mu\text{L}$  of protein solution and 1  $\mu\text{L}$  of precipitant solution is mixed to prepare the crystallization solution, and the droplet of crystallization solution is placed into a well of microplate. The precipitant works to decrease the solubility of proteins. The microplate setting the crystallization droplet is stored at the appropriate temperature until forming the protein crystals. For example, the hanging drop crystallization method is the most widely used for primary screening. Characteristics of the method is that supersaturation of the crystallization solution is gradually increased by the water-vapor diffusion from the crystallization droplet to precipitant solution in the reservoir during incubation. Diffusion rate of the water-vapor and the time necessary for reach the equilibrium can control by the mixing ratio of protein and precipitant solutions. When the appropriate kinds and concentration of precipitant solution is selected, protein crystals form in the droplet by increasing supersaturation of crystallization solution. However, protein crystals do not form at the suitable crystallization condition. Therefore, the optimization of protein crystallization condition is the first barrier of the protein crystallization.

A nucleation of protein crystal occurs at the high supersaturation condition by adding the precipitant solution. However, the moderate supersaturation condition is preferable for the crystal growth, because the high supersaturation condition lead to increase lattice defects. This is a major dilemma of protein crystallization process to control the nucleation and crystal growth [62, 63].

X-ray diffraction experiment is also essential part of the protein crystallography. Proteins are crystallized with hydrated water molecules, the percentage of water molecules occupy 50% w/w in average. Thus, manipulation of the protein crystals for the X-ray diffraction experiment difficult due to the fragility of protein crystals. In addition, cryoprotection process to prevent the deterioration of protein crystals during the X-ray diffraction experiment is also important for protein crystallography. Current synchrotron facilities enabled X-ray diffraction data collection from the micrometer-sized crystals by high energy and photon flux X-ray beam [64, 65]. However, the high energy X-ray beam caused the radiation damage during the measurement process. To avoid the X-ray radiation damage, protein crystal undergoes the cryoprotection and is measured at 100 K in cold nitrogen gas stream [66, 67]. Optimization of cryoprotection condition and damage-less cryoprotection procedure are indispensable for high quality X-ray diffraction data. Finally, the protein three dimensional structure is determined from the X-ray diffraction data using a PC.

A variety of the microfluidic devices have been developed for protein crystallography, which realize the effective crystallization condition screening, growth control of the protein crystals, on-chip X-ray diffraction measurement, membrane protein crystallography, time-resolved protein crystallography. Basically, microfluidic devices for protein crystallography was miniaturization of the conventional technique. However, the applications of microfluidic devices for protein crystallography have been expanding by the advances of the synchrotron facilities.

### 2.3 Microfluidic Devices for High-Throughput Screening of Protein Crystallization Condition

Screening of protein crystallization condition is the one of the most significant problems in protein crystallography. Screening for hundreds or thousands of protein crystallization condition is necessary to prepare diffraction quality protein crystals. In the case of the conventional protein crystallization screening, a robotic system equipped with an automatic liquid dispenser is employed for high-throughput screening. For example, mosquito<sup>®</sup> supplied from TTP LabTech Ltd. is a major automated dispenser [56]. The pipetting range of sample is tens of nano litter to micro litter, and the typical microplate is useable for the screening experiment. However, these kinds of automated dispenser are astonishingly expensive, and require a constant running cost.

In comparison with the conventional methods, microfluidic devices provide many advantages for protein crystallization screening. Figure 2.2 shows the droplet-based high-throughput screening system of protein crystallization condition [43]. Ismagilov's group first reported the droplet-based protein crystallization system. Protein, precipitant, buffer, and additives (PEG) were separately introduced into the microchannel, and droplets containing the all reagent at the defined concentration were continuously generated by shearing the oil flow stream. The composition of

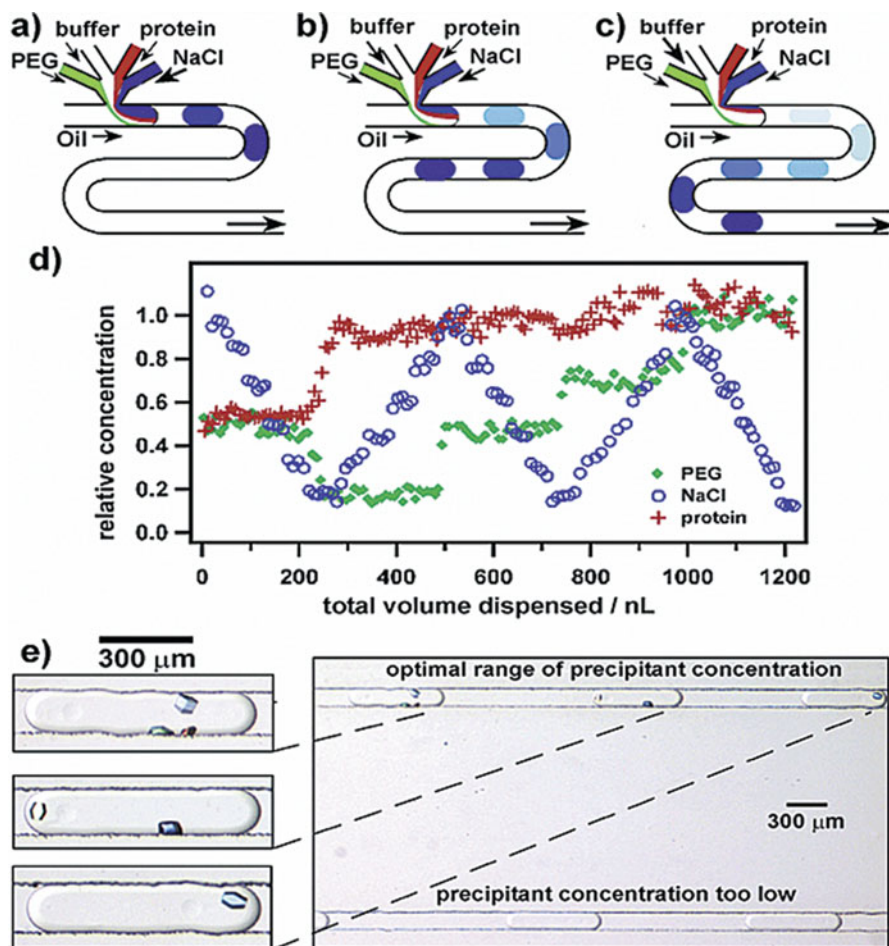


**Fig. 2.2** Droplet-based high-throughput protein crystallization condition screening system. (a–c) A schematic illustration of generation process of microdroplets including protein, NaCl, PEG, and buffer. When the flow rate of NaCl is decreased and the flow rate of buffer solution is increased, the supersaturation condition of the droplet is decreased. (d) Characterization of the idea shown in (a–c). Flow rate of oil was 12 nL/s. Flow rates of aqueous solutions of PEG, salt, lysozyme, and acetate buffer were varied between 0.8 and 5 nL/s. The total flow rate of the aqueous solutions was set at 15 nL/s. (e) Photographs of lysozyme crystals appeared in the droplets of variable composition. (Reprinted with permission from Ref. [43] with permission from The American Chemical Society)

each reagent was defined by initial concentration of solutions and flow rates. When the flow rate of NaCl was gradually decreased as shown in Fig. 2.2a–c, tens of droplets containing different concentration of NaCl were automatically generated in several seconds. The droplet volume was picoliter to nanoliter order and controlled by the flow conditions. Figure 2.2d shows relative concentration of each reagent within the droplets. Protein crystals formed at the optimal crystallization condition ranges (Fig. 2.2e).

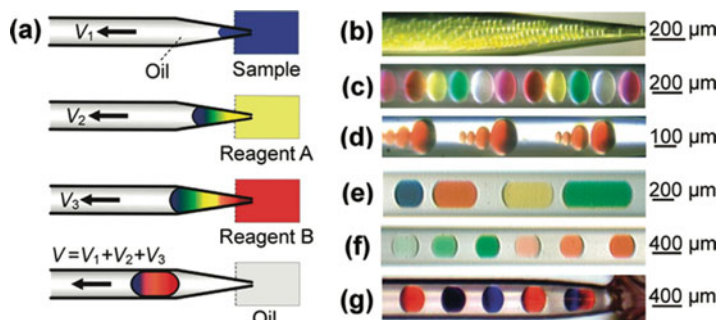


**Fig. 2.3** (a) Schematic illustration of droplet formation process. (b) Continuous droplet generation of 20 pL volume at a throughput of 4.5 s per droplet by sequentially aspirating a 20 pL fluorescence solution and 80 pL of oil at flow rates of 2 and 8 nL/min. (c) Continuous generation of 1.6 nL droplets containing five different dyes. (d) Droplets with different volumes of 20, 40, 160, and 1000 pL. (e) Droplets generation with different volumes (2.5, 4.5, 5.5, and 8.0 nL) and different kinds of dyes. (f) Droplets of 2.5 nL volume with concentration gradient formed by diluting the green and red dye solutions. (g) 2.5 nL droplets formed by sequentially introducing red dye, water, and blue dye with different mixing ratios. The mixing ratios were 1.0:1.5:0, 0.5:1.5:0.5, and 0:1.5:1.0. (Reprinted with permission from Ref. [68] with permission from The American Chemical Society)

An automated microfluidic droplets formation platform named DropLab has been developed by Fang's group. Schematic illustrations of droplets formation using DropLab system is shown in Fig. 2.3 [68]. The minimum droplet volume using the DropLab was  $\sim 20$  pL and the operation speed was 4.5 s per droplet. The concentration gradient between droplets was able to form by changing the dispensing ratio of each reagent. Figure 2.4 shows the protein crystallization condition screening and the optimization experiments using the DropLab system. In the case of crystallization condition screening, 50 droplets with 12 nL containing different precipitant and concentration solution in each were arrayed in a 10 cm long capillary within 22.5 min. As shown in Fig. 2.4a–c, lysozyme crystals were appeared at the suitable precipitant condition. Then, the optimization of the mixing ratio between the 100 mg/mL lysozyme solution and precipitant #1 (1.0 M NaCl and 25% PEG 6000 in 0.1 M sodium acetate buffer (pH 4.6)) were carried out to define the best crystallization condition (Fig. 2.4d–e). Forty droplets array with different mixing ratios of lysozyme to precipitants #1 were generated similarly with precipitant screening.

The droplets which are 5 kinds of mixing ratios of lysozyme to precipitant with 4:1, 2:1, 1:1, 1:2, and 1:4, were prepared in a 10 droplet sequence. The best lysozyme crystals were obtained at the mixing ratio of 1:2 (4 nL lysozyme and 8 nL precipitant #1).

A microwell-based protein crystallization platform is first reported by Quake's group in 2002 [47]. In the case of microwell-based crystallization platform, introduction of sample solutions is carried out by pneumatic valve operation [69]. They fabricated the protein crystallization device enabled 144 parallel condition screening. The microfluidic device was made from PDMS and sealed with glass substrate.

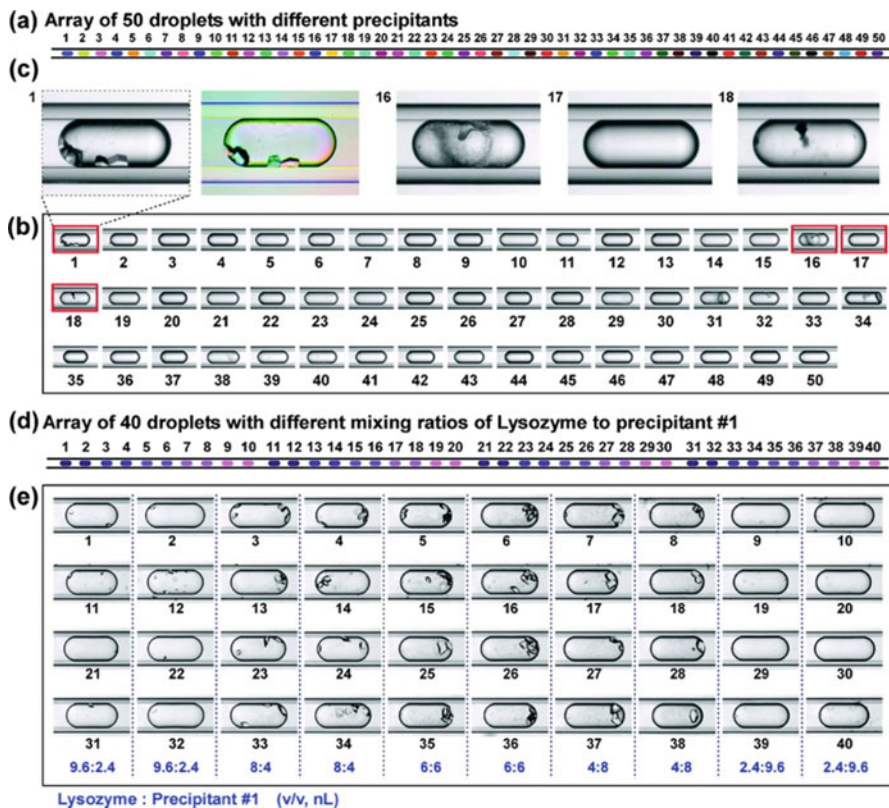


**Fig. 2.4** Lysozyme crystallization screening using DropLab. **(a)** Schematic illustration of droplet array for lysozyme crystallization condition screening using 50 different precipitants. **(b)** Photographs of 50 droplets containing lysozyme and 50 different precipitants in the droplet array of one capillary after a 20 h incubation. **(c)** Enlarged views of droplets containing precipitant #1, #16, #17, and #18 in **(b)**. Lysozyme crystals were obtained in droplet #1. The second image of droplet #1 is a polarized microphotograph. **(d)** Schematic illustration droplet array for optimization of mixing ratio of protein to precipitant #1. **(e)** Photographs of 40 droplets (4 duplicates) in the droplet array with different mixing ratios of 4:1, 2:1, 1:1, 1:2, and 1:4 between lysozyme and precipitant #1. Droplet volume was 12 nL. (Reprinted with permission from Ref. [68] with permission from The American Chemical Society)

Different volume ratio of protein solutions and precipitant solutions were filled separately to microwells via the normally closed valve. After introducing each solution, the valves at the middle section (mixing valve) were opened to mix the protein and precipitant solutions by interface diffusion. This crystallization method is called as “free interface diffusion” in the field of protein crystallography. The protein and precipitant solutions were gradually mixed by molecular diffusion, thus the supersaturation of the solution can control by the opening time of mixing valve. This type of microfluidic device enabled comprehensive protein crystallization condition screening by only pipetting the protein and precipitant solutions at each



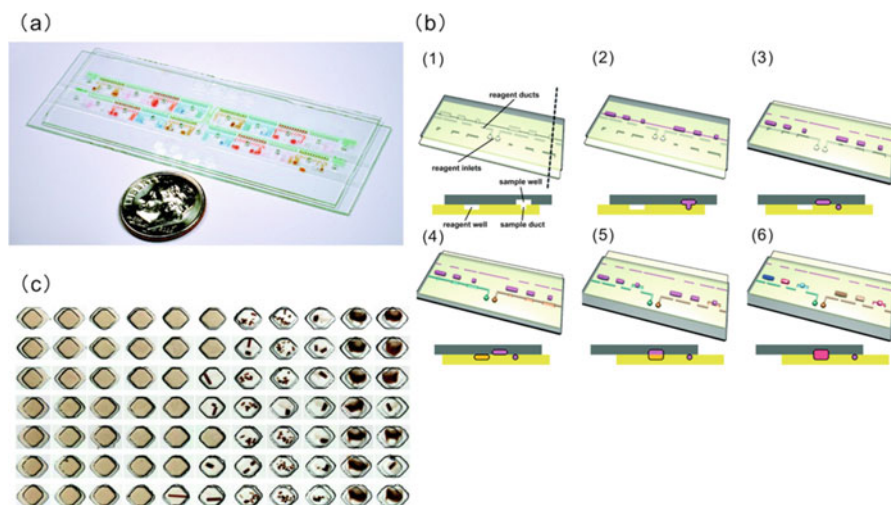


**Fig. 2.5** (a) Photograph of SlipChip. (b) Schematic illustrations of reagent-loading procedure. (c) Screening of the photosynthetic reaction center using SlipChip. 11 trials using the same precipitant at different concentration ratios were demonstrated. (Reprinted with permission from Ref. [45] with permission from The American Chemical Society)

inlet. The optimal protein and precipitant concentration are simultaneously explored by the different volume ration of microwell sets and mixing time of the solutions. Six different proteins such as, lysozyme, bacterial primase catalytic core domain, type-II topoisomerase, thaumatin, xylanase, and glucose isomerase were crystallized using the microfluidic device. In addition, a thaumatin crystal collected from the micro wells (5 nL volume) after appearing the crystal were analyzed by X-ray diffraction experiment and a high-resolution diffraction pattern is observed. This result suggests that microwell platform was able to grow a diffraction quality protein crystal as well as screening of the protein crystallization condition.

A unique protein crystallization condition screening device was reported from Ismagilov's group [45, 70]. The microfluidic device was named as "SlipChip". Figure 2.5 shows the schematic illustration of the SlipChip and its operating photographs. Protein solution was loaded into the microchannel (bottom side) and microwells (upper side) followed by slipped to divide the microchannel and microwells (Fig. 2.5a–c). Then, precipitant solution was loaded into the other microchannel and microwells, and the substrates are additionally slipped to mix the solutions. There were also fabricated different sized microwells to realize the high-throughput protein crystallization screening. Basically, the crystallization principle of SlipChip was free-interface diffusion like microwell-based device mentioned above. They applied SlipChip to determine the crystal structure of glutaryl-CoA dehydrogenase and dihydrofolate reductase/thymidylate synthase. These proteins are diffracted at the resolution of 1.6 Å and 1.9 Å, for glutaryl-CoA dehydrogenase and dihydro-folate reductase/thymidylate synthase, respectively. SlipChip

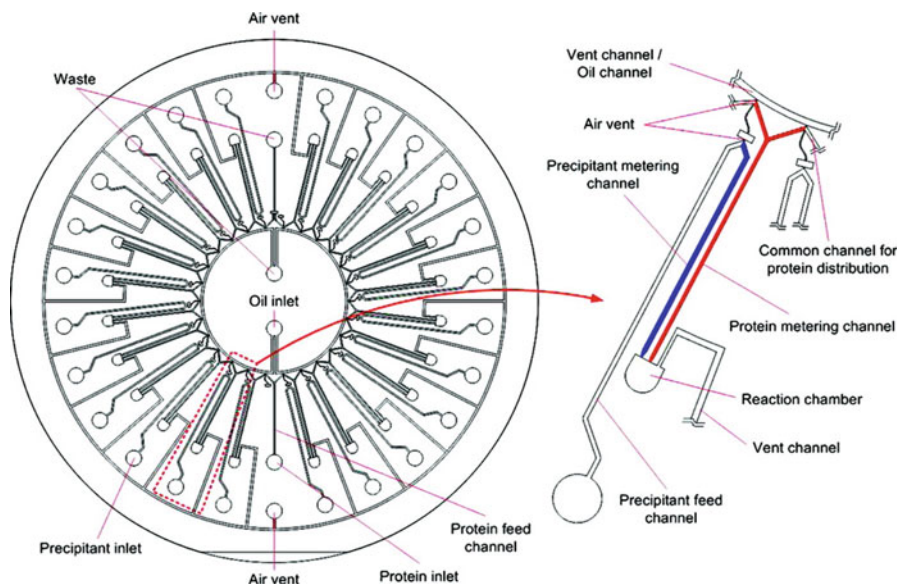


**Fig. 2.6** Schematic illustrations of centrifugal microfluidic device with 24 crystallization array. The device has 24 parallel microstructure units. Each unit comprises a protein metering structure, a precipitant metering structure, and a crystallization chamber. All protein metering structures are connected via a common channel to the sample inlet, and each precipitant metering structure is connected via a feed channel to an individual inlet. Outlets of both the protein metering channel and the precipitant channel are connected to the crystallization chamber. (Reprinted with permission from Ref. [72] with permission from The American Chemical Society)

provide us the simple operation for protein crystallization screening, although the mass productivity of device is lower than that of PDMS-based microfluidic devices.

Centrifugal microfluidic devices are also used for protein crystallography [71, 72]. Wang et al. demonstrated the 24 parallel protein crystallization experiment with one operation using a single microfluidic device (Fig. 2.6). The microfluidic device was made from PDMS microchannel and glass substrate. They tested the protein crystallization using lysozyme, xylanase, lipase B, glucose isomerase, and thermolysin. A protein solution and precipitant solutions were introduced each chamber by centrifugal and capillary force. Each chamber set of protein and precipitant solution were connected with microchannels. Therefore, the microfluidic device was able to employ the vapor diffusion crystallization method. The supersaturation of protein solution was gradually increased by water vapor diffusion similar with the conventional hanging drop vapor diffusion method. For the lysozyme crystallization, the microfluidic device got lysozyme crystals at 81 different conditions. This result indicates the hits rate of the vapor diffusion chip is same as the conventional hanging drop vapor diffusion method (76 hits). However, the vapor diffusion chip allowed the rapid experimental setup (6–8 min for vapor diffusion chip, and 20–30 min for the conventional hanging drop vapor diffusion method) and reduction of sample consumption (6 nL/trial for vapor diffusion chip, and 2  $\mu$ L/trial for the conventional vapor diffusion method).

## 2.4 Protein Crystal Growth in a Microspace Environment

Microfluidic device is useful for not only the protein crystallization condition screening, but also the preparation of high quality protein crystal. When the optimized protein crystallization is founded by the primary screening, improving the quality of protein crystal is addressed by additional optimization of crystallization condition screening. Typically, high diffraction quality protein crystals are not necessarily obtained even with the crystallization condition is optimized. The high diffraction quality crystal is defined as a good molecular packing single crystal (not multiple or aggregated crystals), and it lead to obtain high quality X-ray diffraction data. Crystallization environment is significant factor to prepare the ordered molecular packing protein crystal. In the case of the ground-based protein crystallization experiment, the natural convection is the main factor of the formation of disordered crystal. From these reasons, protein crystallization experiments at a special environment: a microgravity (at the International Space Station), a magnetic field, or an electric field have been reported [33, 34]. These environments make it possible to suppress the natural convection and the offer a diffusion-controlled protein crystal growth environment. Microspace environments: the microdroplet and the microwell are alternative ground-based crystallization platforms of the special crystallization environment. In this section, microfluidic platforms for preparation of high diffraction crystal is introduced.

Advantages of the microspace environment on the protein crystallography are producing one single crystal in a microdroplet or microwell (single crystallization) and controlling protein crystal shape suitable for X-ray crystal structure analysis [55–57, 73, 74]. Single crystallization is a technique for preventing an aggregation of protein crystals to obtain high quality X-ray diffraction data. When a number of nucleus or crystals formed in the crystallization droplet, each protein crystal cannot grow enough to obtain good X-ray diffraction data due to the consumption of protein molecules at the nucleation and early stage of crystal growth. In addition, one single crystal must be exposed by X-ray beam to collect the “single crystal X-ray diffraction data”. From the viewpoint of X-ray data collection, stacked or aggregated protein crystals: a needle-like crystal and a cluster-like crystal lowers the diffraction quality and complicates the crystal structure analysis after the diffraction data collection. In the case of these types of crystals, crystal growth control plays important roles to prevent staking of each crystal.

Maeki et al. reported droplet-based protein single crystallization method. They focused on the effect of droplet size on the protein crystallization and elucidated the critical droplet size for generating one single crystal in the microdroplet both theoretically and experimentally [56]. Figure 2.7 shows the concept of the single protein crystallization method based on the microdroplet. After first nucleation of a protein crystal in the droplet, the protein crystal grow in competition with further nucleation until the supersaturation of the solution reaches the metastable region. Thus, a one single crystal was generated in a droplet smaller than the critical droplet size. Conversely, a large size droplet made it possible continuously nucleation rather

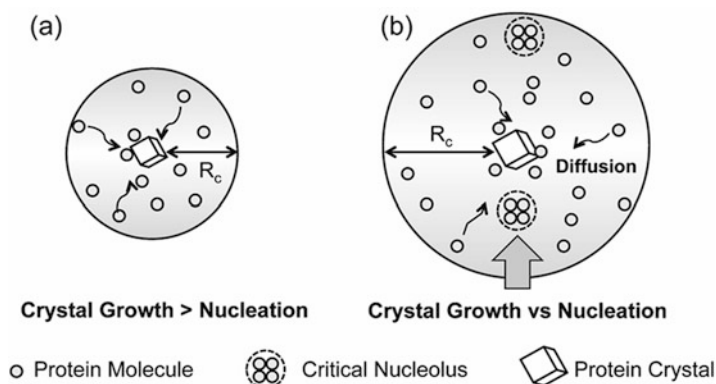


**Fig. 2.7** Droplet-based high-throughput protein crystallization condition screening system. Concept of the single crystallization method based on droplet microfluidics. (a) Droplet size  $< R_c$ . (b) Droplet size  $> R_c$ . The critical size was estimated from the diffusion coefficient, the initial concentration of protein, and the consumption rate of protein in solution. (Reprinted with permission from Ref. [56] with permission from Wiley-VCH)

than the crystal growth after first nucleation. The microdroplet single nucleation method is based on the mass balance of protein molecules and Fick's laws of protein diffusion. The critical droplet ( $R_c$ ) size was able to calculate from the diffusion coefficient of protein molecules ( $D$ ), the initial concentration of protein in the droplet ( $C_0$ ), and the consumption rate of protein by crystal growth ( $q$ ), as shown in the following equation:

$$R_c = (6DC_0/q)^{1/2}$$

To proof of concept, four model proteins: lysozyme (14 kDa), thaumatin (22 kDa), glu cose isomerase (179 kDa, four subunits), and ferritin (440 kDa, 24 subunits) were used for crystallization experiments. The  $R_c$  values were theoretically calculated as 600, 600, 450, and 200  $\mu\text{m}$  for lysozyme, thaumatin, glucose isomerase, and ferritin, respectively. In the case of lysozyme and thaumatin, single crystallization enabled using 200 and 360  $\mu\text{m}$  sized droplets, regardless of the supersaturation condition. On the other hand, multiple crystals formed in the 500  $\mu\text{m}$  sized droplet after first nucleation at the high supersaturation condition. After the first nucleation, protein concentration gradient formed in the microdroplet, regardless of the droplet size, and it have been confirmed by in situ Raman spectroscopy. In other words, high concentration of protein remains in the area far away from the crystal. The protein concentration gradient gradually disappeared by molecular diffusion due to the depletion of protein molecules around the formed crystal. In the case of small-sized droplet, protein molecules could rapidly diffuse and incorporated to the formed crystal compared with the large sized droplet. However, in the case of large sized droplet, although protein molecules diffuse to the formed crystal, the time to necessary to reach the protein molecules to the crystal became long compared with

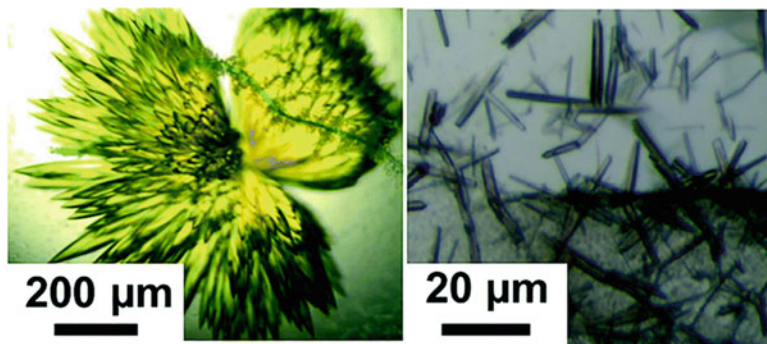


**Fig. 2.8** Photographs of protein crystals unsuitable for single crystal X-ray crystallography grown without microseeds. (left) Photoactive yellow protein (PYP) and (right) cytochrome  $bo_3$  oxidase (cyt  $bo_3$ ). (Reprinted with permission from Ref. [58] with permission from The Royal Society of Chemistry)

the small sized droplet. For this reason, further nucleation enables in the region, which protein molecules remains at high concentration. For the ferritin crystallization, molecular diffusion of ferritin assumed slower than that of the small molecular weight proteins: lysozyme and thaumatin. Therefore, multiple crystals form in the droplet like the lysozyme and thaumatin crystallization using the large sized droplet. These results suggest that a strategy for design of microfluidic devices to control the protein crystallization behavior.

Stacking or aggregating of protein crystals are serious problems in the protein crystallography (Fig. 2.8). Typically, the aggregations lower the diffraction quality and complicates the structure determination process. To avoid the aggregation of protein crystals, crystallization control based on the phase diagram is useful technique both the conventional methods and microfluidic methods. The aggregation occurs by the nucleation onto the surface of protein crystals formed in the crystallization droplet (or well). Thus, protein crystals incubated under the suitable crystallization (supersaturation) condition can avoid the aggregations.

Kenis et al. reported a microseeding method using a microfluidic device [58]. Figure 2.9 shows a microfluidic approach for the protein crystallization experiment using microseed. The microfluidic device composed four layers including PDMS layers (50  $\mu\text{m}$  for one layer) and cyclic olefin copolymer layers (50  $\mu\text{m}$  for one layer). The total thickness of the microfluidic device was 200  $\mu\text{m}$ , which expected good X-ray transmission efficiency. The microfluidic device enabled 24 crystallization trials using 6 different concentration of diluted microseed solutions at once. The solutions: the protein-precipitant solution and the microseed solutions were introduced into the 24 microwells via the normally closed valves and mixed to transport the microseeds to the crystallization solution under the metastable region (Fig. 2.9b). Under the metastable region, protein crystal can grow without further nucleation. Figure 2.9c–d shows the photographs of the crystals of (c) photoactive yellow protein (PYP, soluble protein) and (d) cytochrome  $bo_3$  oxidase (cyt  $bo_3$ , membrane

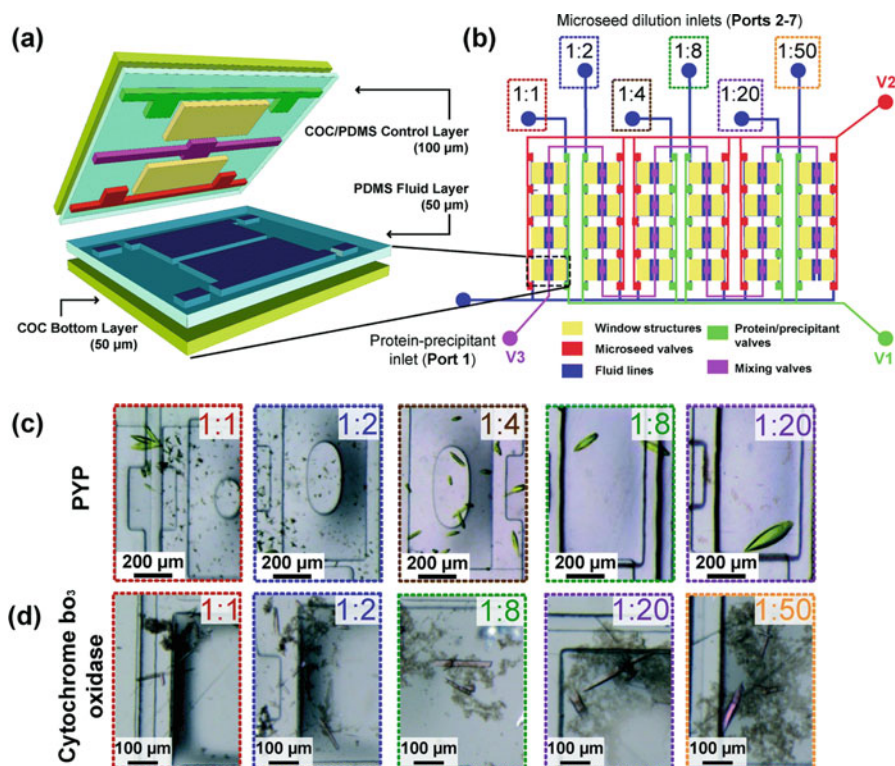


**Fig. 2.9** (a) 3D perspective view of the microfluidic device with normally closed pneumatic valves. The microfluidic device comprised of four layers: an impermeable cyclic olefin copolymer top layer bonded to an PDMS control layer containing valves, a PDMS fluid layer to contain protein, precipitant and seed solutions, and a COC bottom layer. (b) Schematic illustration of a 24-well array chip used for microseeding. Fluid layer is represented in blue, and the valve lines, V1, V2 and V3, are colored based on their function. In the case of microseeding experiments, different microseed dilutions and a pre-mixed protein–precipitant solution were introduced into the device from inlets 2–7 and inlet 1, respectively, prior to on-chip mixing. (c and d) Results of the dilution ratio screening of the seed solutions. At greater seed dilutions (lower seed concentration), PYP crystals (c) grew into fewer, larger crystals and cyt bo<sub>3</sub> crystals (d) grew into fewer, thicker crystals. (Reprinted with permission from Ref. [58] with permission from The Royal Society of Chemistry)

protein). In comparison with the conventional crystallization method shown in Fig. 2.8, the aggregations of protein crystals were able to prevent by the microseeding method using microfluidic device. When the high concentration of microseed solution was used, the small sized crystals formed in the crystallization well. Conversely, 200 and 100 μm sized crystals for PYP and cyt bo<sub>3</sub> were obtained at the low concentration of microseed solution. At the microseeding process, the competition of dissolution of microseeds and growth of microseeds occurs in the crystallization solution and therefore, the appropriate dilution rate of microseed solution allows the crystal growth of one or a few protein crystals in the solution.

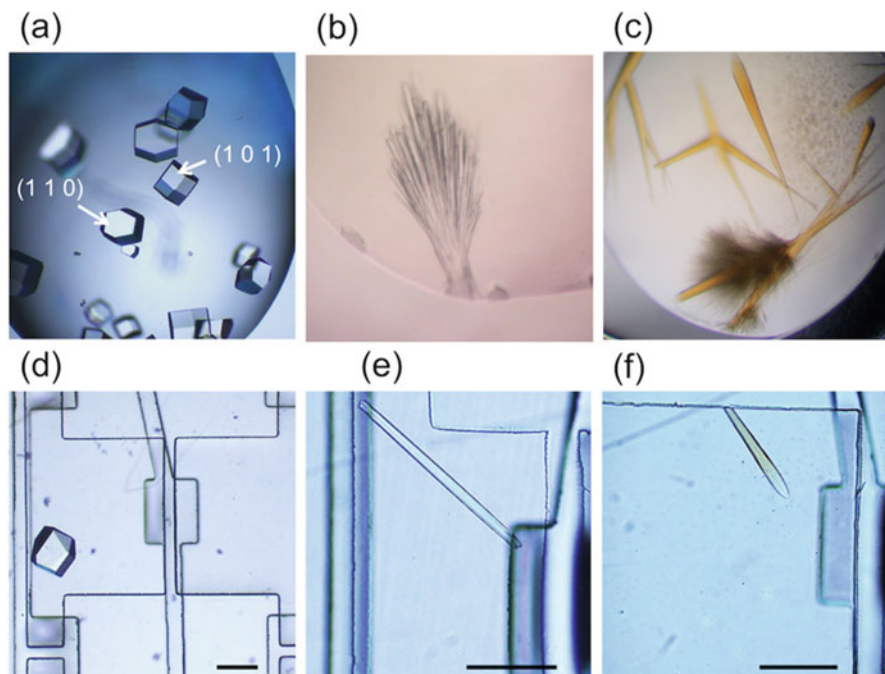


**Fig. 2.10** Photographs of protein crystals formed by the (a) microbatch method, (b, c) hanging drop vapor diffusion method, and the (d–f) microfluidic chip method. (a, d) Lysozyme crystal, (b, e) PsGK crystal, and (c, f) CPR–HO complex crystal. The scale bars represent 200  $\mu\text{m}$ . (Reprinted with permission from Ref. [55] with permission from The Royal Society of Chemistry)

They also optimized the microfluidic system with separated microchannels for protein, precipitant, and microseed solutions to precisely control the mixing of three solutions. By the improved microfluidic device, the microseeds solution was transported to the crystallization solution (mixture of protein and precipitant solution) at preferable time. The resolution of  $\text{bo}_3$  was improved by the microfluidic approach from 12  $\text{\AA}$  to 10  $\text{\AA}$ . Although, the diffraction resolution was not enough to determine the three-dimensional structure, the microfluidic approach expects to become a non-invasive and high throughput optimization method to obtain high diffraction quality protein crystal after the first protein crystallization condition screening.

Maeki et al. found the difference of protein crystal growth behavior depended on the depth of crystallization chamber and demonstrated that the reforming of aggregated protein crystal [55]. They also employed the microseeding method using the microfluidic devices with normally closed valves. Lysozyme, glucokinase from *Pseudoalteromonas* sp. AS-131 (PsGK), and NADPH- cytochrome P450 oxidoreductase-heme oxygenase complex (CPR-HO complex) as model proteins. Figure 2.10 shows the photographs of protein crystals formed by the (a) microbatch method, (b, c) hanging drop vapor diffusion method, and the (d–f) microfluidic

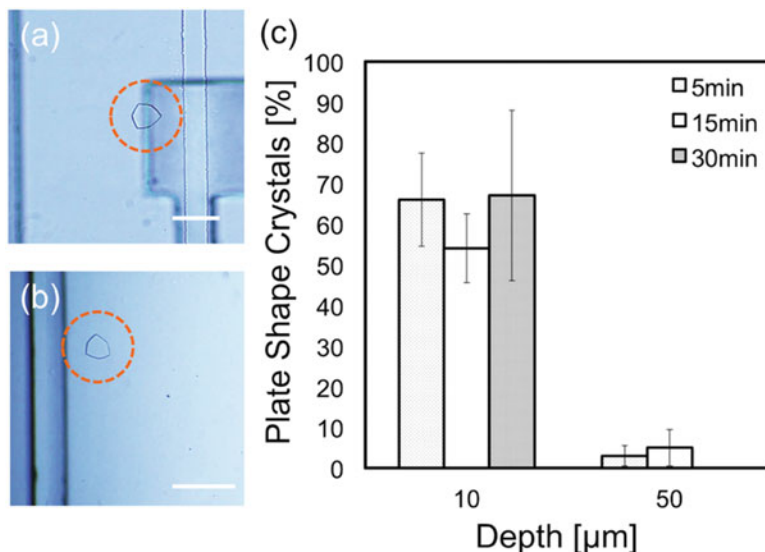


**Fig. 2.11** (a, b) Photographs of the plate-shaped PsGK crystals formed in the microfluidic device with 10 μm deep crystallization chambers. (c) Percentage of the plate-shaped PsGK crystals formed under different mixing times. The scale bars represent 100 μm. (Reprinted with permission from Ref. [55] with permission from The Royal Society of Chemistry)

devices. This result indicates that the microseeding method coupled with the microfluidic device was a universal protein crystallization control technique. In addition, they demonstrated the shape of PsGK crystal was dramatically changed by the depth of the crystallization chamber. Although, the rod-shaped PsGK crystal formed in 50 μm depth microfluidic device, the plate-shaped PsGK crystal formed in 10 μm depth microfluidic device, as shown in Fig. 2.11. Mixing time (5–30 min) between the crystallization solution and the microseed solution did not affect the crystal shape. The three-dimensional structure of PsGK have been determined by the rod-shaped crystal formed by the conventional hanging drop vapor diffusion method. Then the plate shaped PsGK crystal was also measured by the X-ray beam at synchrotron facility. The plate shaped PsGK crystal diffracted at a resolution limit of 2.8 Å and the crystallographic parameters: the space group and the lattice constant were same as the rod-shaped PsGK crystal. For the X-ray diffraction measurement, the plate-shaped crystal is easy to irradiate the X-ray beam on the targeted crystal, because the irradiation area of crystal is larger than that of the rod-shaped crystal. The thick cubic-shaped crystal provides the high diffraction intensity and ideally is the best for the X-ray single crystallography. Theoretically, the plate-shaped crystal can grow to the cubic-shaped crystal by the additional macroseeding method. Therefore, the reforming method followed by the macroseeding may offer the solution for the preparation of high diffraction quality crystal.



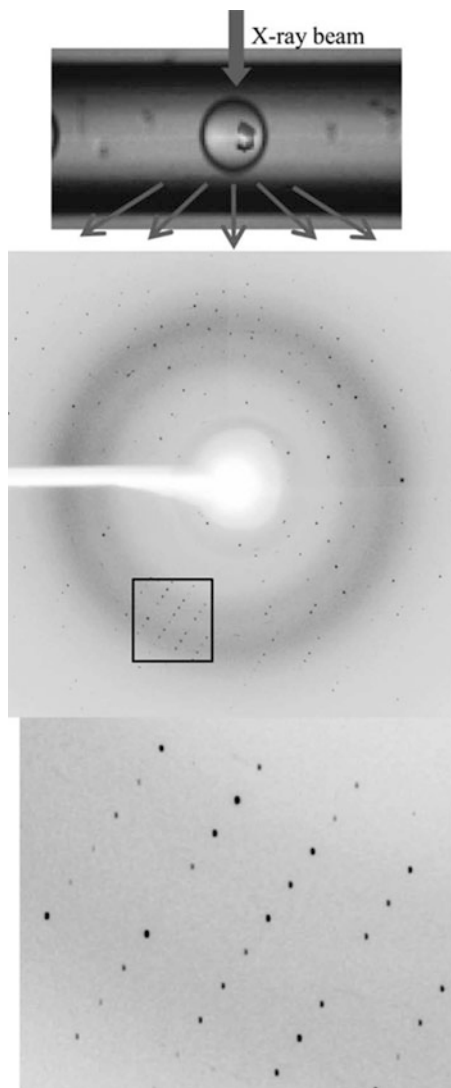
## 2.5 On-Chip Protein Crystal Structure Analysis and Other Applications

X-ray diffraction measurement is the last experimental step on the protein crystallography. When the X-ray diffraction data is obtained, the three-dimensional protein structure is calculated using a personal computer or a super computer. The size of protein crystals obtained by the microfluidic device is typically smaller than 200  $\mu\text{m}$  due to the limitation of crystallization space (microdroplet or microwell). Thus, a synchrotron facility is widely employed for the X-ray diffraction measurement. Generally, X-ray diffraction measurement is carried out at the cryogenic condition to reduce the radiation damage. The room-temperature measurement also enables, if the diffraction data collected from the different protein crystals is able to merge each other. Advances in X-ray free electron laser (XFEL), the serial femtosecond X-ray crystallography at room temperature will be indispensable technique for elucidating the protein structures and dynamics [75–78]. In any cases, optimization and selection of the quality of protein crystals, characteristics of microfluidic device (material and thickness), and the characteristic of X-ray beam (photon flux and beam spot size) requires to collect high quality diffraction data.

Microfluidic devices for both of the on-chip X-ray measurements at cryogenic and room temperature conditions have been reported in several papers. For the on-chip X-ray measurement, the suitable substrate materials should be selected to reduce the background signal. In addition, the thickness of the microfluidic device also affects the X-ray diffraction intensity. Ismagilov et al. demonstrated that *in situ* X-ray analysis using microdroplets collected into the glass capillary with 200  $\mu\text{m}$  inner, and 180  $\mu\text{m}$  outer diameters [79]. Microdroplets containing thaumatin crystal were directly exposed X-ray in 10 s beam at BioCARS station 14BM-C and 14ID-B at the Advanced Photon Source at Argonne National Laboratory (USA). Thaumatin crystals diffracted to 1.8  $\text{\AA}$  resolution and the crystallographic parameters are the same as the reported thaumatin crystal prepared by the conventional crystallization method. The background signal from the glass capillary is enough to low, because they used 10  $\mu\text{m}$  thickness-wall glass capillary. Teflon or PFA (perfluoroalkoxy alkane) capillary (I. D. 200  $\mu\text{m}$ , O. D. 360  $\mu\text{m}$ , 80  $\mu\text{m}$  wall thickness) was also acceptable for the device material to determine the crystallographic parameters: lattice constant and space group (BL 07 in the SAGA Light Source, Japan) (Fig. 2.12) [80]. However, the background signal at the small angle was slightly higher than that of thin-wall glass capillary. These results suggest that the thinner microfluidic device is desirable for obtaining high signal to noise ratio X-ray diffraction data by on-chip measurement.

X-ray compatible COC-PDMS hybrid microfluidic device was developed by Kenis's group [52]. They evaluated the effect of substrate materials and thickness on the X-ray transmission and confirmed that the COC-PDMS device showed the transmission factor was more than 90%. Then, they carried out X-ray measurement

**Fig. 2.12** (top) Lysozyme crystal formed in the microdroplet within capillary. (middle and bottom) X-ray diffraction patterns obtained by directly irradiation of X-ray to the lysozyme crystal within the capillary. (Reprinted with permission from Ref. [80] with permission from The Japan Society for Analytical Chemistry)



using lysozyme crystal at room temperature in the oscillation range from  $-5^\circ$  to  $+5^\circ$  ( $10^\circ$  per one lysozyme crystal,  $1^\circ$  oscillation step with 1 s exposure). Diffraction data from multiple lysozyme crystals were merged to obtain a complete data set. The diffraction data was compared with the lysozyme crystal prepared by the conventional crystallization method over the resolution range from 50 Å to 1.55 Å. The lysozyme crystal prepared by the conventional method underwent cryoprotection to obtain a complete diffraction data set. The quality of the diffraction data using the microfluidic device was compatible with the conventional crystallization and analytical method. Maeki et al. first demonstrated the integration of protein

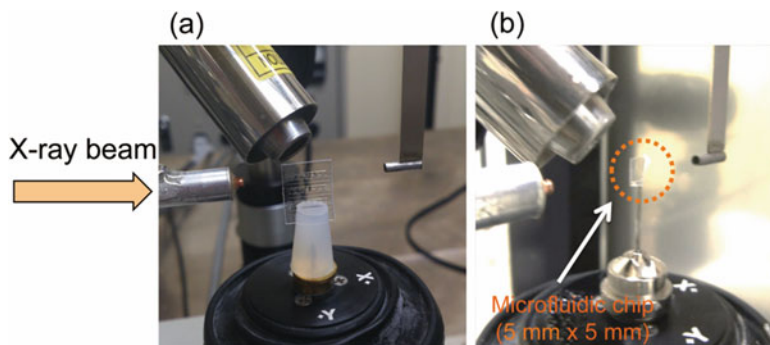


**Fig. 2.13** Comparison of the cooling situation of the microfluidic chip by cold nitrogen gas. (a) Photograph of the in situ X-ray diffraction experiment using a standard microfluidic chip at 277 K. (b) Photograph of a microfluidic chip that was cut to a size of  $5 \times 5 \text{ mm}^2$ . This microfluidic chip was used for the X-ray diffraction experiment at 100 K. (Reprinted with permission from Ref. [81] with permission from The American Chemical Society)

crystallization to on chip X-ray diffraction procedure including cryoprotection [81]. Figure 2.13 shows the photographs of the X-ray diffraction experiment setup: at (a) 277 K and (b) 100 K (cryogenic condition). They also used the COC-PDMS microfluidic ( $240 \mu\text{m}$  thickness) device with normally closed pneumatic valves to mix the cryoprotectant after appearing lysozyme crystals in microwells. The standard microfluidic device ( $3 \times 4 \text{ cm}^2$ ) was not completely placed in the cold nitrogen stream and the crystals formed in the device could not apply the flash cooling. In contrast, the microfluidic device optimized for the cryoprotection enabled the flash cooling process and obtained complete diffraction data set from one protein single crystal (oscillation range:  $0^\circ$  to  $90^\circ$ ,  $1^\circ$  oscillation step with 30 s exposure at BL 07 in the SAGA Light Source, Japan). They can avoid the X-ray radiation damage by the cryoprotection and the lysozyme crystal diffracted to  $1.5 \text{ \AA}$  resolution and the three-dimensional structure was determined from one single crystal. The microfluidic device with normally closed valves made it possible the step-wise cryoprotection to reduce the osmotic shock at the cryoprotection. The stepwise cryoprotection induced the improvement of diffraction data quality.

Perry et al. developed a graphene-based microfluidic device to reduce the background signal. Figure 2.14 shows schematic illustrations of fabrication and operation procedures [82]. Unlike the polymer-based materials, the thickness of single layer graphene is sub-nanometer. Therefore, the signal to noise ratio is expected extremely increase, because of the decreasing of the background signal. They confirmed that the  $100 \mu\text{m}$  thick COC layer increased the attenuation and background scatter [83]. Typically, micro crystals show the low diffraction intensity compared with large-sized crystals, thus the graphene-based microfluidic device is useful for the micro-crystallography. In addition, the graphene-based microfluidic device can be applied not only for the X-ray crystallography and also the other analytical methods including small angle X-ray diffraction (SAXS) and cryo-transmission electron microscopy (cryo-TEM) to analyze the biological targets.

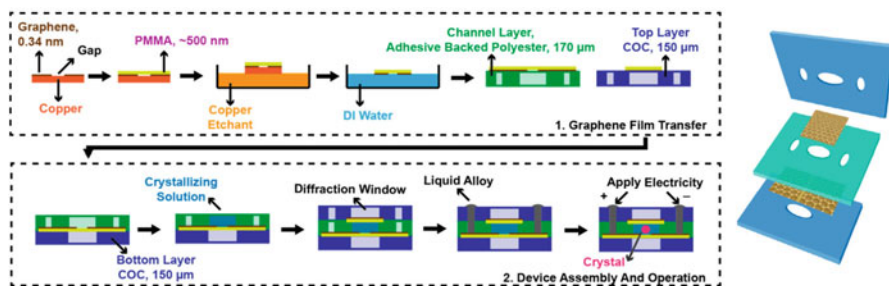
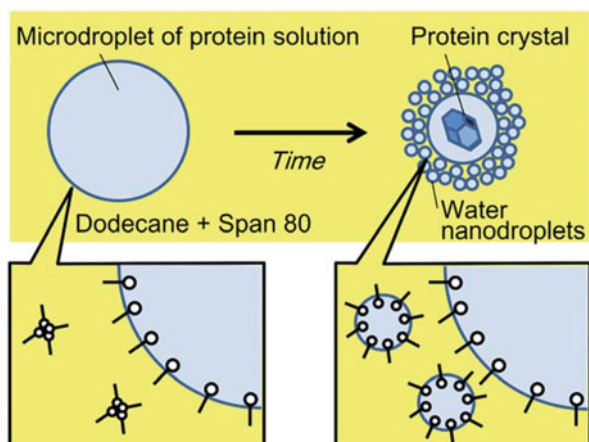


**Fig. 2.14** Schematic illustrations of the device fabrication and operation procedures. A graphene membrane on copper is coated with a layer of PMMA, and then released from the copper substrate by etching. The graphene-PMMA film is floated on the surface of water and transferred to an adhesive polyester support layer. This layer is adhered to a COC layer containing the cut-out pattern for the microfluidic channels. Assembled device is held together by the adhesive layers defining the window structures. (Reprinted with permission from Ref. [82] with permission from MDPI)

**Fig. 2.15** Concept of microdroplet-based protein crystallization using spontaneous emulsification. (Reprinted with permission from Ref. [84] with permission from The Royal Society of Chemistry)



Fukuyama et al. reported a droplet-based vapor diffusion protein crystallization method [84]. They focused on the spontaneous emulsification to increase the supersaturation in microdroplets. Figure 2.15 shows the concept of microdroplet-based protein crystallization using spontaneous emulsification. They used lysozyme as a model protein and microdroplets containing a crystallization solution: a mixture of lysozyme and precipitant were dispersed into a continuous phase (Dodecane + Span 80). The supersaturation in the microdroplets are gradually increased by the spontaneous emulsification. When a 60 mM Span 80 solution was used as the continuous phase, the microdroplet was shrunk 180  $\mu\text{m}$  to 100  $\mu\text{m}$  within 35 min. The increasing rate of supersaturation was able to control by the concentration of Span 80. Vapor diffusion method is most widely used protein crystallization method in the conventional methods. The supersaturation is increased to reach the equilibrium to reservoir solution with increasing the incubation time. Therefore, the

crystallization condition is explored in wide supersaturation range. The microdroplet-based vapor diffusion method provides many advantages in protein crystallography by reducing the protein sample consumption and high-throughput crystallization condition screening compared with the typical microdroplet-based protein crystallization method.

## 2.6 Summary

This chapter summarized that the microfluidic techniques and platforms for protein crystallography. Microfluidics has a great potential in the protein crystallographic applications: high-throughput protein crystallization condition screening, low amount of sample consumption, high quality single crystal preparation, and on-chip X-ray diffraction measurement. A number of nano or picoliter-scale trials are prepared by simple operation compared with the conventional crystallization methods. In addition, the quality of protein crystals is able to improve using the microfluidic device and environment without special apparatus. On-chip X-ray crystallography using micro and nano protein crystals will be main research topic, because of the recent advances of synchrotron facility. In particular, microfluidic devices coupled with XFELs certainly accelerate the protein three dimensional structure analysis. Novel microfluidic-based techniques and devices for protein crystallography will be developed along with the progress of synchrotron facility and diffraction data and statistical processing.

## References

1. Nilsson J, Ståhl S, Lundeberg J, Uhlén M, Per-Å (1997) Affinity fusion strategies for detection, purification, and immobilization of recombinant proteins. *Protein Expr Purif* 11:1–16
2. Arnau J, Lauritzen C, Petersen GE, Pedersen J (2006) Current strategies for the use of affinity tags and tag removal for the purification of recombinant proteins. *Protein Expr Purif* 48:1–13
3. Maeki M, Kimura N, Sato Y, Harashima H, Tokeshi M (2018) Advances in microfluidics for lipid nanoparticles and extracellular vesicles and applications in drug delivery systems. *Adv Drug Deliv Rev* 128:84–100
4. Mazaafrianto D, Maeki M, Ishida A, Tani H, Tokeshi M (2018) Recent microdevice-based Aptamer sensors. *Micromachines* 9(5):202
5. Gong MM, Sinton D (2017) Turning the page: advancing paper-based microfluidics for broad diagnostic application. *Chem Rev* 117:8447–8480
6. Osaki T, Takeuchi S (2017) Artificial cell membrane systems for biosensing applications. *Anal Chem* 89:216–231
7. Armbrrecht L, Dittrich PS (2017) Recent advances in the analysis of single cells. *Anal Chem* 89:2–21
8. Wu J, Chen Q, Lin JM (2017) Microfluidic technologies in cell isolation and analysis for biomedical applications. *Analyst* 142:421–441
9. Hao SJ, Wan Y, Xia YQ, Zou X, Zheng SY (2018) Size-based separation methods of circulating tumor cells. *Adv Drug Deliv Rev* 125:3–20

10. Kaminski TS, Garstecki P (2017) Controlled droplet microfluidic systems for multistep chemical and biological assays. *Chem Soc Rev* 46:6210–6226
11. Kurita R, Niwa O (2016) Microfluidic platforms for DNA methylation analysis. *Lab Chip* 16:3631–3644
12. Strohmeier O, Keller M, Schwemmer F, Zehnle S, Mark D, von Stetten F, Zengerle R, Paust N (2015) Centrifugal microfluidic platforms: advanced unit operations and applications. *Chem Soc Rev* 44:6187–6229
13. Gutmann B, Cantillo D, Kappe CO (2015) Continuous-flow technology—a tool for the safe manufacturing of active pharmaceutical ingredients. *Angew Chem Int Ed Eng* 54:6688–6728
14. Suryawanshi PL, Gumpfekar SP, Bhanvase BA, Sonawane SH, Pimplapure MS (2018) A review on microreactors: reactor fabrication, design, and cutting-edge applications. *Chem Eng Sci* 189:431–448
15. Shi HH, Xiao Y, Ferguson S, Huang X, Wang N, Hao HX (2017) Progress of crystallization in microfluidic devices. *Lab Chip* 17:2167–2185
16. Shembekar N, Chaipan C, Utharala R, Merten CA (2016) Droplet-based microfluidics in drug discovery, transcriptomics and high-throughput molecular genetics. *Lab Chip* 16:1314–1331
17. Dittrich PS, Manz A (2006) Lab-on-a-chip: microfluidics in drug discovery. *Nat Rev Drug Discov* 5:210–218
18. Sesen M, Alan T, Neild A (2017) Droplet control technologies for microfluidic high throughput screening (muHTS). *Lab Chip* 17:2372–2394
19. Venkatakrishnan AJ, Deupi X, Lebon G, Tate CG, Schertler GF, Babu MM (2013) Molecular signatures of G-protein-coupled receptors. *Nature* 494:185–194
20. Surade S, Blundell TL (2012) Structural biology and drug discovery of difficult targets: the limits of ligandability. *Chem Biol* 19:42–50
21. Nooren IMA, Thornton JM (2003) Diversity of protein-protein interactions. *EMBO J* 22:3486–3492
22. Knowles TP, Vendruscolo M, Dobson CM (2014) The amyloid state and its association with protein misfolding diseases. *Nat Rev Mol Cell Biol* 15:384–396
23. Lonsdale R, Ward RA (2018) Structure-based design of targeted covalent inhibitors. *Chem Soc Rev* 47:3816–3830
24. Wang SH, Yu J (2018) Structure-based design for binding peptides in anti-cancer therapy. *Biomaterials* 156:1–15
25. Ferreira LG, Dos Santos RN, Oliva G, Andricopulo AD (2015) Molecular docking and structure-based drug design strategies. *Molecules* 20:13384–13421
26. Blundell TL, Jhoti H, Abell C (2002) High-throughput crystallography for lead discovery in drug design. *Nat Rev Drug Discov* 1:45–54
27. Liu W, Wacker D, Gati C, Han GW, James D, Wang D, Nelson G, Weierstall U, Katritch V, Barty A, Zatsepin NA, Li D, Messerschmidt M, S.b. Boutet GJ, Williams JE, Koglin MM, Seibert C, Wang STA, Shah S, Basu R, Fromme C, Kupitz KN, Rendek I, Grotjohann P, Fromme RA, Kirian KR, Beyerlein TA, White HN, Chapman M, Caffrey JCH, Spence RC, Stevens VC (2013) Serial femtosecond crystallography of G protein-coupled receptors. *Science* 342:1521–1524
28. Rosenbaum DM, Rasmussen SG, Kobilka BK (2009) The structure and function of G-protein-coupled receptors. *Nature* 459:356–363
29. Hong M, Zhang Y, Hu F (2012) Membrane protein structure and dynamics from NMR spectroscopy. *Annu Rev Phys Chem* 63:1–24
30. Cheng Y, Grigorieff N, Penczek PA, Walz T (2015) A primer to single-particle cryo-electron microscopy. *Cell* 161:438–449
31. Russo Krauss I, Merlini A, Vergara A, Sica F (2013) An overview of biological macromolecule crystallization. *Int J Mol Sci* 14:11643–11691
32. McPherson A, DeLucas LJ (2015) Microgravity protein crystallization. *NPJ Microgravity* 1:15010

33. Kundrot CE, Judge RA, Pusey ML, Snell EH (2001) Microgravity and macromolecular crystallography. *Cryst Growth Des* 1:87–99
34. Pareja-Rivera C, Cuéllar-Cruz M, Esturau-Escofet N, Demitri N, Polentarutti M, Stojanoff V, Moreno A (2016) Recent advances in the understanding of the influence of electric and magnetic fields on protein crystal growth. *Cryst Growth Des* 17:135–145
35. Li F, Lakerveld R (2018) Electric-field-assisted protein crystallization in continuous flow. *Cryst Growth Des* 18:2964–2971
36. Koizumi H, Uda S, Fujiwara K, Tachibana M, Kojima K, Nozawa J (2015) Crystallization of high-quality protein crystals using an external electric field. *J Appl Crystallogr* 48:1507–1513
37. Sazaki G, Yoshida E, Komatsu H, Nakada T, Miyashita S, Watanabe K (1997) Effects of a magnetic field on the nucleation and growth of protein crystals. *J Cryst Growth* 173:231–234
38. Shang L, Cheng Y, Zhao Y (2017) Emerging droplet microfluidics. *Chem Rev* 117:7964–8040
39. Hibara A, Fukuyama M, Chung M, Priest C, Proskurnin MA (2016) Interfacial phenomena and fluid control in micro/nanofluidics. *Anal Sci* 32:11–21
40. Beebe DJ, Mensing GA, Walker GM (2002) Physics and applications of microfluidics in biology. *Annu Rev Biomed Eng* 4:261–286
41. Di Carlo D (2009) Inertial microfluidics. *Lab Chip* 9:3038–3046
42. Li L, Ismagilov RF (2010) Protein crystallization using microfluidic technologies based on valves, droplets, and slipchip. *Annu Rev Biophys* 39:139–158
43. Zheng B, Roach LS, Ismagilov RF (2003) Screening of protein crystallization conditions on a microfluidic chip using nanoliter-size droplets. *J Am Chem Soc* 125:11170–11171
44. Maeki M, Yamaguchi H, Tokeshi M, Miyazaki M (2016) Microfluidic approaches for protein crystal structure analysis. *Anal Sci* 32:3–9
45. Li L, Du W, Ismagilov R (2010) User-loaded slipchip for equipment-free multiplexed nanoliter-scale experiments. *J Am Chem Soc* 132:106–111
46. Li L, Mustafi D, Fu Q, Tereshko V, Chen DL, Tice JD, Ismagilov RF (2006) Nanoliter microfluidic hybrid method for simultaneous screening and optimization validated with crystallization of membrane proteins. *Proc Natl Acad Sci U S A* 103:19243–19248
47. Hansen CL, Skordalakes E, Berger JM, Quake SR (2002) A robust and scalable microfluidic metering method that allows protein crystal growth by free interface diffusion. *Proc Natl Acad Sci U S A* 99:16531–16536
48. Hansen CL, Classen S, Berger JM, Quake SR (2006) A microfluidic device for kinetic optimization of protein crystallization and in situ structure determination. *J Am Chem Soc* 128:3142–3143
49. Heymann M, Ophthalage A, Wierman JL, Akella S, Szebenyi DM, Gruner SM, Fraden S (2014) Room-temperature serial crystallography using a kinetically optimized microfluidic device for protein crystallization and on-chip X-ray diffraction. *IUCrJ* 1:349–360
50. Shim J-u, Cristobal G, Link DR, Thorsen T, Jia Y, Piattelli K, Fraden S (2007) Control and measurement of the phase behavior of aqueous solutions using microfluidics. *J Am Chem Soc* 129:8825–8835
51. Talreja S, Kim DY, Mirarefi AY, Zukoski CF, Kenis PJA (2005) Screening and optimization of protein crystallization conditions through gradual evaporation using a novel crystallization platform. *J Appl Crystallogr* 38:988–995
52. Guha S, Perry SL, Pawate AS, Kenis PJ (2012) Fabrication of X-ray compatible microfluidic platforms for protein crystallization. *Sensors Actuators B Chem* 174:1–9
53. Khvostichenko DS, Schieferstein JM, Pawate AS, Laible PD, Kenis PJ (2014) X-ray transparent microfluidic chip for mesophase-based crystallization of membrane proteins and on-chip structure determination. *Cryst Growth Des* 14:4886–4890
54. Liang YR, Zhu LN, Gao J, Zhao HX, Zhu Y, Ye S, Fang Q (2017) 3D-printed high-density droplet array chip for miniaturized protein crystallization screening under vapor diffusion mode. *ACS Appl Mater Interfaces* 9:11837–11845

55. Maeki M, Yamazaki S, Pawate AS, Ishida A, Tani H, Yamashita K, Sugishima M, Watanabe K, Tokeshi M, Kenis PJA, Miyazaki M (2016) A microfluidic-based protein crystallization method in 10 micrometer-sized crystallization space. *CrystEngComm* 18:7722–7727
56. Maeki M, Teshima Y, Yoshizuka S, Yamaguchi H, Yamashita K, Miyazaki M (2014) Controlling protein crystal nucleation by droplet-based microfluidics. *Chem Eur J* 20:1049–1056
57. Yamaguchi H, Maeki M, Yamashita K, Nakamura H, Miyazaki M, Maeda H (2013) Controlling one protein crystal growth by droplet-based microfluidic system. *J Biochem* 153:339–346
58. Schieferstein JM, Pawate AS, Varel MJ, Guha S, Astrauskaite I, Gennis RB, Kenis PJA (2018) X-ray transparent microfluidic platforms for membrane protein crystallization with microseeds. *Lab Chip* 18:944–954
59. Zhang S, Gerard CJJ, Ikni A, Ferry G, Vuillard LM, Boutin JA, Ferte N, Grossier R, Candoni N, Veessler S (2017) Microfluidic platform for optimization of crystallization conditions. *J Cryst Growth* 472:18–28
60. Ildelfonso M, Candoni N, Veessler S (2011) Using microfluidics for fast, accurate measurement of lysozyme nucleation kinetics. *Cryst Growth Des* 11:1527–1530
61. Grossier R, Magnaldo A, Veessler S (2010) Ultra-fast crystallization due to confinement. *J Cryst Growth* 312:487–489
62. Vekilov PG (2010) Nucleation. *Cryst Growth Des* 10:5007–5019
63. Vekilov PG (2007) What determines the rate of growth of crystals from solution? *Cryst Growth Des* 7:2796–2810
64. Moukhametzianov R, Burghammer M, Edwards PC, Petitdemange S, Popov D, Fransén M, McMullan G, Schertler GF, Riekel C (2008) Protein crystallography with a micrometre-sized synchrotron-radiation beam. *Acta Crystallogr D Biol Crystallogr* 64:158–166
65. Yamamoto M, Hirata K, Yamashita K, Hasegawa K, Ueno G, Ago H, Kumasaka T (2017) Protein microcrystallography using synchrotron radiation. *IUCrJ* 4:529–539
66. Berejnov V, Hussein NS, Alsaied OA, Thorne RE (2006) Effects of cryoprotectant concentration and cooling rate on vitrification of aqueous solutions. *J Appl Crystallogr* 39:244–251
67. Pflugrath JW (2004) Macromolecular cryocrystallography--methods for cooling and mounting protein crystals at cryogenic temperatures. *Methods* 34:415–423
68. Du W-B, Sun M, Gu S-Q, Zhu Y, Fang Q (2010) Automated microfluidic screening assay platform based on droplab. *Anal Chem* 82:9941–9947
69. Thorsen T, Maerkl SJ, Quake SR (2002) Microfluidic large-scale integration. *Science* 298:580–584
70. Li L, Du W, Ismagilov RF (2010) Multiparameter screening on slipchip used for nanoliter protein crystallization combining free interface diffusion and microbatch methods. *J Am Chem Soc* 132:112–119
71. Wang L, Sun K, Hu X, Li G, Jin Q, Zhao J (2015) A centrifugal microfluidic device for screening protein crystallization conditions by vapor diffusion. *Sensors Actuators B Chem* 219:105–111
72. Li G, Chen Q, Li J, Hu X, Zhao J (2010) A compact disk-like centrifugal microfluidic system for high-throughput nanoliter-scale protein crystallization screening. *Anal Chem* 82:4362–4369
73. Maeki M, Yamaguchi H, Yamashita K, Nakamura H, Miyazaki M, Maeda H (2012) A method for generating single crystals that rely on internal fluid dynamics of microdroplets. *Chem Commun (Camb)* 48:5037–5039
74. Maeki M, Yamaguchi H, Yamashita K, Nakamura H, Miyazaki M, Maeda H (2011) Analysis of kinetic behavior of protein crystallization in nanodroplets. *Chem Lett* 40:825–827
75. Chapman HN, Fromme P, Barty A, White TA, Kirian RA, Aquila A, Hunter MS, Schulz J, DePonte DP, Weierstall U, Doak RB, Maia FR, Martin AV, Schlichting I, Lomb L, Coppola N, Shoeman RL, Epp SW, Hartmann R, Rolles D, Rudenko A, Foucar L, Kimmel N, Weidenspointner G, Holl P, Liang M, Barthelmess M, Caleman C, Boutet S, Bogan MJ, Krzywinski J, Bostedt C, Bajt S, Gumprecht L, Rudek B, Erk B, Schmidt C, Homke A, Reich C, Pietschner D, Struder L, Hauser G, Gorke H, Ullrich J, Herrmann S, Schaller G, Schopper F, Soltau H, Kuhnlel KU, Messerschmidt M, Bozek JD, Hau-Riege SP, Frank M,



- Hampton CY, Sierra RG, Starodub D, Williams GJ, Hajdu J, Timneanu N, Seibert MM, Andreasson J, Rucker A, Jonsson O, Svenda M, Stern S, Nass K, Andritschke R, Schroter CD, Krasniqi F, Bott M, Schmidt KE, Wang X, Grotjohann I, Holton JM, Barends TR, Neutze R, Marchesini S, Fromme R, Schorb S, Rupp D, Adolph M, Gorkhover T, Andersson I, Hirsemann H, Potdevin G, Graafsma H, Nilsson B, Spence JC (2011) Femtosecond X-ray protein nanocrystallography. *Nature* 470:73–77
76. Spence JCH (2017) XFELs for structure and dynamics in biology. *IUCrJ* 4:322–339
77. Suga M, Akita F, Hirata K, Ueno G, Murakami H, Nakajima Y, Shimizu T, Yamashita K, Yamamoto M, Ago H, Shen JR (2015) Native structure of photosystem II at 1.95 Å resolution viewed by femtosecond X-ray pulses. *Nature* 517:99–103
78. Tosha T, Nomura T, Nishida T, Saeki N, Okubayashi K, Yamagiwa R, Sugahara M, Nakane T, Yamashita K, Hirata K, Ueno G, Kimura T, Hisano T, Muramoto K, Sawai H, Takeda H, Mizohata E, Yamashita A, Kanematsu Y, Takano Y, Nango E, Tanaka R, Nureki O, Shoji O, Ikemoto Y, Murakami H, Owada S, Tono K, Yabashi M, Yamamoto M, Ago H, Iwata S, Sugimoto H, Shiro Y, Kubo M (2017) Capturing an initial intermediate during the P450<sub>nor</sub> enzymatic reaction using time-resolved XFEL crystallography and caged-substrate. *Nat Commun* 8:1585
79. Zheng B, Tice JD, Roach LS, Ismagilov RF (2004) A droplet-based, composite PDMS/glass capillary microfluidic system for evaluating protein crystallization conditions by microbatch and vapor-diffusion methods with on-chip X-ray diffraction. *Angew Chem Int Ed Engl* 43:2508–2511
80. Maeki M, Yoshizuka S, Yamaguchi H, Kawamoto M, Yamashita K, Nakamura H, Miyazaki M, Maeda H (2012) X-ray diffraction of protein crystal grown in a nano-liter scale droplet in a microchannel and evaluation of its applicability. *Anal Sci* 28:65–68
81. Maeki M, Pawate AS, Yamashita K, Kawamoto M, Tokeshi M, Kenis PJ, Miyazaki M (2015) A method of cryoprotection for protein crystallography by using a microfluidic chip and its application for in situ X-ray diffraction measurements. *Anal Chem* 87:4194–4200
82. Sui S, Wang Y, Dimitrakopoulos C, Perry S (2018) A graphene-based microfluidic platform for electrocrystallization and in situ X-ray diffraction. *Crystals* 8
83. Sui S, Wang Y, Kolewe KW, Srajer V, Henning R, Schiffman JD, Dimitrakopoulos C, Perry SL (2016) Graphene-based microfluidics for serial crystallography. *Lab Chip* 16:3082–3096
84. Fukuyama M, Akiyama A, Harada M, Okada T, Hibara A (2015) Microfluidic protein crystallisation controlled using spontaneous emulsification. *Anal Methods* 7:7128–7131